

Evidence of the torsion of a polyene chain in a strongly hindered molecular environment: The ttbP4 crystal

Javier Catalán^{a,*}, Ana Martin-Somer^{a,*}, Henning Hopf^b

^a Departamento de Química Física Aplicada, Universidad Autónoma de Madrid, 28049 Madrid, Spain

^b Technische Universität Braunschweig, Institut für Organische Chemie, Hagenring 30, D-38106 Braunschweig, Germany

ARTICLE INFO

Keywords:

Polyene photochemistry
Simulation of vibronic spectra
DFT calculations

ABSTRACT

In this work we provide experimental and theoretical evidence that in a molecular environment as restricted as the crystalline phase, the all-trans ttbP4 (1,1,8,8-tetrakis(*tert*-butyl)octa-1,3,5,7-tetraene) can undergo a conformational change, by rotating around the second single bond, when it is electronically excited to its 1^1Bu state. Undoubtedly, this is an interesting step to clarify the viability of the torsional mechanism of retinal pigments in the cavity of bacteriorhodopsin as proposed in the vision mechanism.

We show that the fluorescence emission of ttbP4 in the crystalline phase is the combination of two bands corresponding to the emission from two different ttbP4 conformers. Theoretical simulations of absorption and emission spectra allowed us to identify the two conformers as: i) the most stable all-trans ttbP4, giving rise to a structured fluorescence band, and ii) the conformer generated by the torsion around the second single bond of ttbP4 polyene chain, giving rise to an emission band with hardly any structure.

Interestingly, experimental data also show that the rotated structure, after deactivating to the ground state, takes a time to return to the all-trans configuration.

1. Introduction

Polyene compounds play a crucial role in natural photophysical processes such as vision [1–3] and photosynthesis [4,5]; they are also part of provitamin A [6], play a relevant role in the color of many vegetables and fruits, and act as natural antioxidants [7,8].

The spectroscopic behavior of these compounds has also helped to establish relevant scientific insights, such as the theory of color in Organic Chemistry [9], or the effect of resonance in unsaturated molecular structures [10]. They have also been relevant in the formulation of chemical-physical models such as the bicycle pedal [11] or the hula-twist process [12–14], which have been used to understand the torsion of the polyene chain of the retinal pigments within the rhodopsin and bacteriorhodopsin cavity in the proposed mechanism for vision [15–17].

Additionally, polyene compounds show a unique photophysical behavior difficult to rationalize. Most of the research done has focused on the study of diphenylpolyenes [18–20]. However, it is worth noting the novel photophysical insights achieved through the study of tetra-*tert*-butyl polyenes (ttbPX, being X the number of double bonds of the polyene chain) [21–25]. The last are non photolabile compounds [24,25] with a planar molecular structure that in contrast with

diphenylpolyenes [26,27], have the twisting of their terminal groups hindered by the *tert*-butyl groups (see Scheme 1).

In previous studies of the photophysical behavior in solution of ttbP4 [24] and ttbP5 [25] polyenes, we have shown that their fluorescence is a combination of bands arising from different structures assigned to a no *all-trans* configuration. These new structures are, in principle, generated by a rotation around a single or double bond of their polyene chain in the excited electronic state [24,25].

In order to provide evidence on the structural changes undergone by rhodopsin chromophores during the vision mechanism, in this study we investigate the structural changes of a polyene molecule, ttbP4, within a molecular environment with strong spatial constrictions, the crystalline phase. With this aim, we studied experimentally and theoretically, whether the rotation of ttbP4 polyene chain upon light absorption that happens in solution also occurs in crystalline samples. Furthermore, we studied if ttbP4 structural changes upon light absorption are reversible after the molecule has deactivated to the ground state, regenerating in this way the original *all-trans* structure.

* Corresponding author.

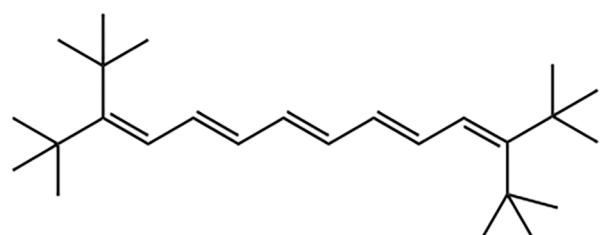
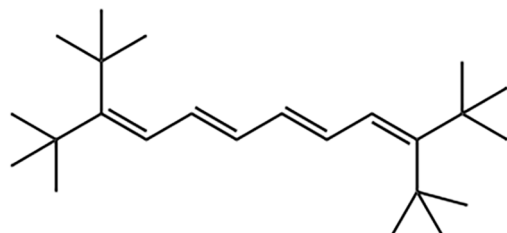
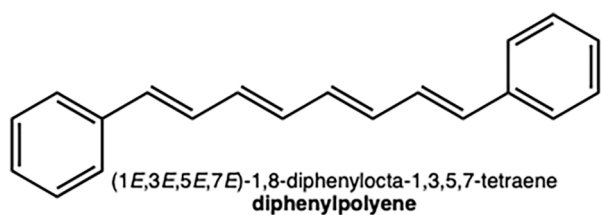
E-mail addresses: javier.catalan@uam.es (J. Catalán), ana.somer@uam.es (A. Martin-Somer).

<https://doi.org/10.1016/j.jphotochem.2023.114679>

Received 11 January 2023; Received in revised form 23 February 2023; Accepted 8 March 2023

Available online 11 March 2023

1010-6030/© 2023 The Author(s). Published by Elsevier B.V. This is an open access article under the CC BY-NC-ND license (<http://creativecommons.org/licenses/by-nc-nd/4.0/>).



Scheme 1. Molecular structures of polyene compounds mentioned in the manuscript: an example of diphenylpolyene (top) and two tetra-tertbutyl polyenes with four (ttbP4, middle) and five (ttbP5, bottom) double bonds in the polyene chain.

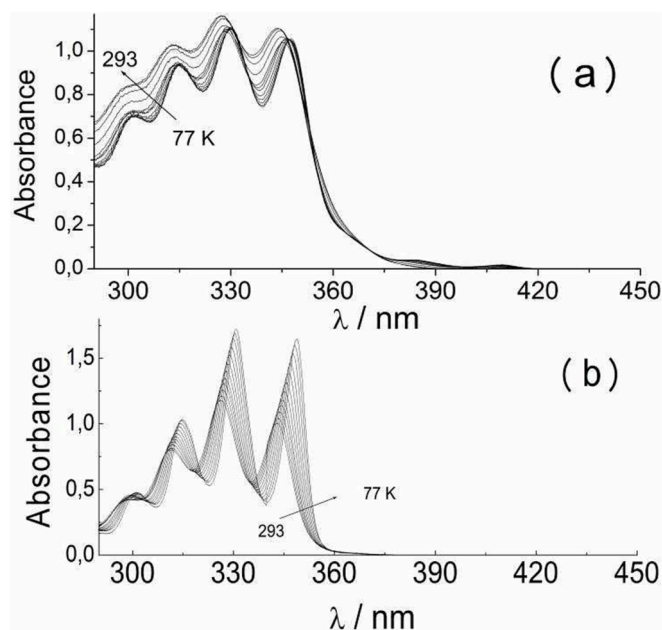


Fig. 1. (a) Absorption bands of crystalline ttbP4 (4tmC) and (b) a solution of ttbP4 in DECMCH (9×10^{-6} M) obtained at temperatures between 293 and 77 K.

2. Experimental and computational methods

2.1. Synthetic procedure

Methanol and dichloromethane were purchased from Merck Uvasol grade. Anhydrous decalin, and methylcyclohexane were purchased from Aldrich, and possess a purity higher than 99%. The all-trans-octatetraene 3,10-di(*tert*-butyl)-2,2,11,11-tetramethyl-3,5,7,9-dodecatetraene(IUPAC-nomenclature, ttbP4, see Scheme 1) has been synthesized in our laboratory [24,26].

The crystallization of ttbP4 was carried out in the dark, allowing a very slow evaporation of the solvent (15 days aprox.) using a 1/1 methanol / dichloromethane mixture. We detected that single crystals are generated in triclinic forms. These small single crystals are selected using a Leica GZ6 optical microscope.

The ttbP4 solutions studied are in a 1/1 mixture of decalin and methylcyclohexane, which we will call DECMCH. This mixture has been chosen for allowing adequate solubility of ttbP4 by lengthening its polyene chain and also maintaining adequate spectral transparency throughout the temperature range studied. A more detailed justification for the choice of this solvent will be reported in another publication.

2.2. Instrumentation

In our experiments the sample temperatures were controlled with an Oxford DN1704 cryostat that was purged with dried nitrogen (99.99% pure) and equipped with an ITC4 controller interfaced to the spectrometers. The ttbP4 single crystals are mounted on a supplied swivel bracket to run on the Oxford DN1704 cryostat.

The UV/Vis absorption spectra were recorded on a Cary-5 spectrophotometer and the emission spectra on an Aminco-Bowman AB2 spectrofluorimeter. In both equipments using a sample holder that was fixed to the cryostat where the ttbP4 single crystal is mounted.

Corrected fluorescence spectra were obtained on a calibrated Aminco – Bowman AB2 spectrofluorimeter. The sensitivity factors for the emission channel, which included not only those depending on the detector, but also those related to the emission monochromator and optical arrangement —channel emission included—, were obtained by using the FP-123 correction kit from SLM Instruments. This required mounting a standard lamp in a channel at right angles to the emission channel in an OL 254 M spectral irradiance lamp from Optronic Laboratories. The lamp was operated at a constant voltage supplied by an SP-270 power source and its light output was driven into an integrating sphere with a pinhole leading to the fluorimeter emission channel. The conversion factors thus obtained were used to convert measured spectra into absolute spectra, which are independent of the specific instrument used.

2.3. Spectra simulation

For the simulation of vibrationally resolved absorption and emission spectra of the studied systems, we optimized and computed the vibrational frequencies of each molecular structure in the ground state by DFT while Time-Dependent density functional theory (TD-DFT) has been utilized for excited states. We used PBE0 [28] hybrid functional and performed the harmonic analysis of the ground and excited state surfaces, around their respective equilibrium structures, checking that the computed frequencies are all positive. PBE0 functional was used in combination with the def2-TZVP basis set as implemented in the Gaussian16 [29] software package. The PBE0 functional was employed for the main part of the analysis, because it has been found to give reasonably accurate spectral lineshapes in previous studies of similar systems [30]. The excited-state properties have been computed using the time-dependent density functional theory (TD-DFT) with the same functional and basis set. All calculations were performed for the gas-phase. The vibrationally resolved absorption spectra were simulated

Table 1

Values for 0–0 transition at different temperatures for crystalline ttbP4 (4tmC) and a solution of ttbP4 in DECMCH (9×10^{-6} M).

Temperature [K]	ttbP4 in DECMCH		4tmC (crystal)	
	cm ⁻¹	nm	cm ⁻¹	nm
293	29097,9	343,67	29093,4	343,72
273	29062,7	344,08	29060,5	344,11
253	29028,5	344,49	29021,7	344,57
213	28958,7	345,32	28950,3	345,42
193	28918,4	345,80	28908,9	345,91
173	28873,2	346,34	28867,4	346,41
153	28842,7	346,71	28846,0	346,67
133	28816,4	347,02	28813,5	347,06
113	28797,4	347,25	28794,2	347,29
93	28784,5	347,41	28787,2	347,38
77	28772,4	347,56	28764,9	347,65

within the harmonic and Franck-Condon approximations employing the FCclasses3 program [31].

3. Results and discussion

We will begin by determining the corresponding UV/Vis absorption spectra of crystalline form of ttbP4, which we will call 4tmC, decreasing temperature from 293 to 77 K. By analyzing the UV/Vis absorption spectra of 4tmC together with spectra obtained in a solution of ttbP4 in DECMCH we will try to show the spectroscopic changes that the crystallization of the compound entails. With this, we will try to support the planarity of the *all-trans* structure of ttbP4 in its ground electronic state, in the wide range of temperatures considered. Later, we will obtain the emission spectra of the crystalline form of ttbP4 (4tmC) between 293 and 77 K. Finally, we will simulate, by means of electronics structure calculations, the theoretical absorption and emission spectra of all the possible conformers of ttbP4 (*all-trans* and structures generated by rotations around single and double bonds). From these analyses we will study the viability of the proposed rapid structural changes in the first excited electronic state of ttbP4, which implies the twisting of its polyene chain in a very spatially restricted medium, comparable to the

protein cavity where the chromophores involved in the process of vision are found.

3.1. Photophysics of 4tmC

In Fig. 1 we show the UV/Vis absorption spectra of (a) 4tmC and (b) a solution of ttbP4 in DECMCH obtained between 293 and 77 K. The value for the 0–0 transition at the different temperatures for both ttbP4 in DECMCH solution and crystalline 4tmC are given in Table 1.

An analysis of these spectra shows a significantly different spectroscopic behavior depending on the state of matter. In solution we observe the typical behavior of diphenylpolyenes and tetra-tertbutyl polyenes (ttbPX), a bathochromic shift and hyperchromic effect of the absorption bands when decreasing sample temperature (Fig. 1b). However, the spectra registered in the crystalline phase (Fig. 1a) show a significantly lower hyperchromic effect. It is also interesting to note the presence of some small absorption signals around 410, 385 and 360 nm, that will be addressed later.

In Fig. 2a we jointly show the bathochromic shift of ttbP4 solution in DECMCH (*) and of the crystalline form, 4tmC (●), when decreasing the temperature from 293 to 77 K. It is important to remark that the displacements found for ttbP4 are about half of those measured for diphenylpolyenes under identical conditions [32]. The smaller bathochromic shifts found for ttbP4 point to a more rigid planar structure compared to the corresponding diphenyl polyene. This observation agrees with X-ray diffraction experiments [33] showing that ttbP4 crystallizes in the triclinic system and exhibits a coplanar octatetraene chain.

Fig. 2b shows the corresponding hyperchromic effect of ttbP4 in solution (*). For the crystalline form there is practically no effect throughout the entire range of temperatures considered, another factor indicating that 4tmC keeps being planar throughout the whole temperature range.

Fig. 3 displays the emission spectra obtained by exciting 4tmC at 300 nm in the temperature range from 293 to 213 K. We observe the presence of a structured fluorescence in the 340–440 nm region. This spectral structure is reminiscent of its UV/Vis absorption spectrum (Fig. 1a).

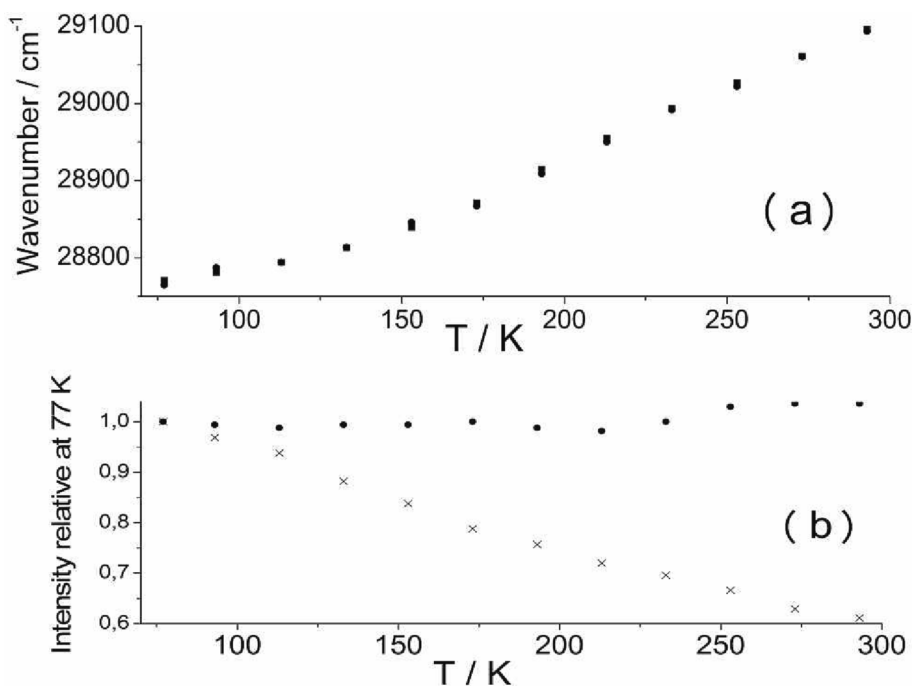


Fig. 2. (a) Bathochromic shift of ttbP4 in a 9×10^{-6} M DECMCH solution (*) and crystalline ttbP4 (4tmC) (●) (b) Corresponding hyperchromic effect for decreasing temperature from 293 K to 77 K.

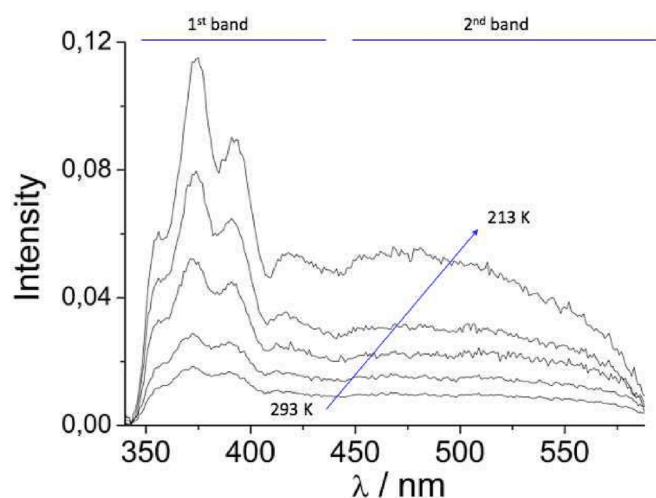


Fig. 3. Emission spectra of 4tmC between 293 and 213 K, exciting at 300 nm. The intensity of the signal increases when decreasing temperature from 293 K to 213 K.

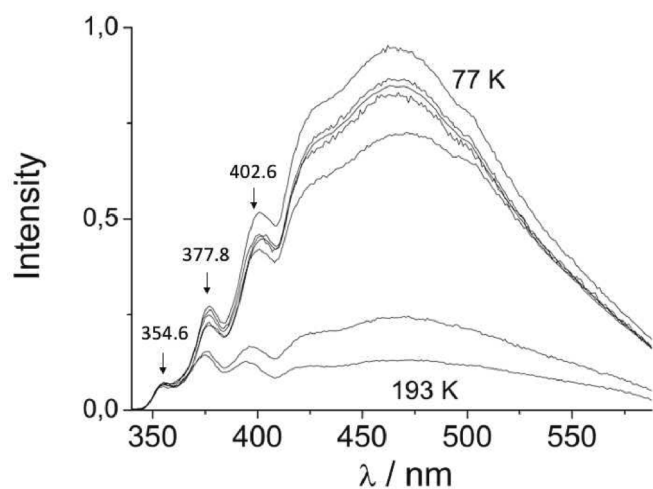


Fig. 4. Emission spectra of 4tmC obtained decreasing temperature from 193 to 77 K, exciting 4tmC at 300 nm.

As the sample is cooled down (from 293 K to 213 K) the intensity of the fluorescence signal increases. In addition, the vibrational structure of the fluorescence band is better defined when the temperature decreases. This signal can, in principle, be assigned to the emission from the 1^1Bu state. This state is the one assigned to the intense first absorption band of the compound [34]. Furthermore, as the temperature decreases, a second fluorescence signal appears in the region beyond 440 nm. This second band has lower intensity than the first band and no apparent structure.

As the temperature continues to decrease (193 K to 77 K, see Fig. 4), the intensity of the band located beyond 440 nm increases and this band becomes clearly dominant. This fluorescence coincides with the fluorescence shown by the compound in a solution in squalane (SQ), see Fig. 8 of reference 24. Therefore, based on the results in reference 24, we suggest that this fluorescence is due to a new ttBP4 structure generated by the rotation of its polyene chain.

If we look now to the excitation spectra of 4tmC (Fig. 5), obtained by recording the fluorescence emission as a function of the wavelength of the excitation light, we can confirm that the fluorescence signals in Figs. 3 and 4 are generated by 4tmC. The emission observed between 340 and 440 nm is mostly assignable to the planar *all-trans*-molecular

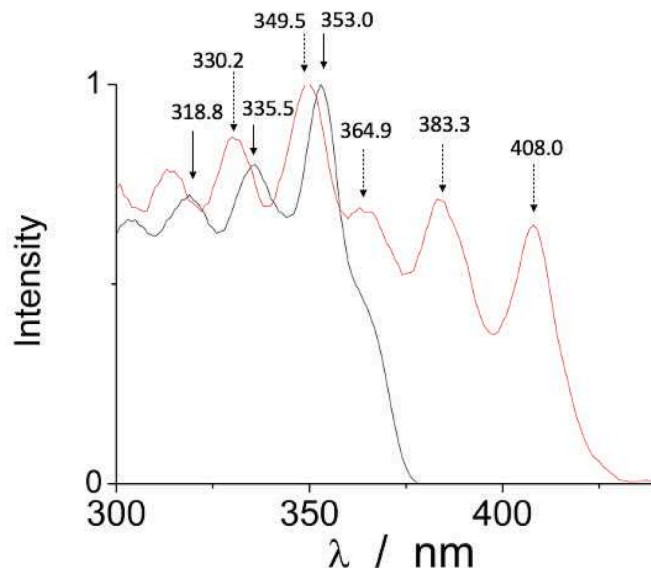


Fig. 5. Normalized fluorescence excitation spectra of 4tmC obtained by i) monitoring light at 400 nm and 77 K (black) and ii) monitoring light at 520 nm and 93 K (red). (For interpretation of the references to color in this figure legend, the reader is referred to the web version of this article.)

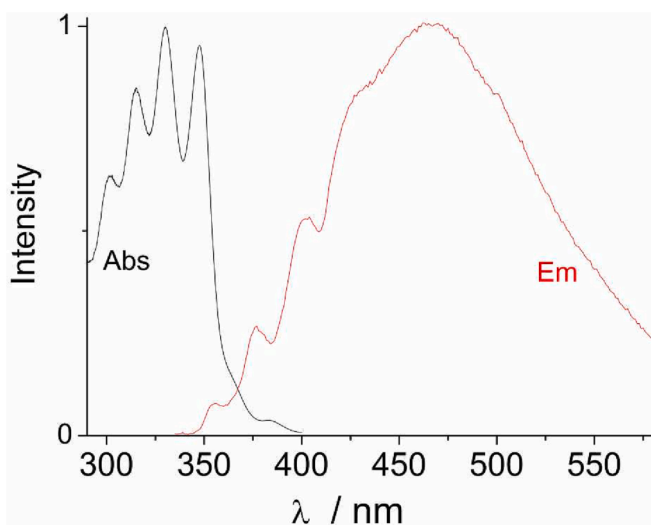
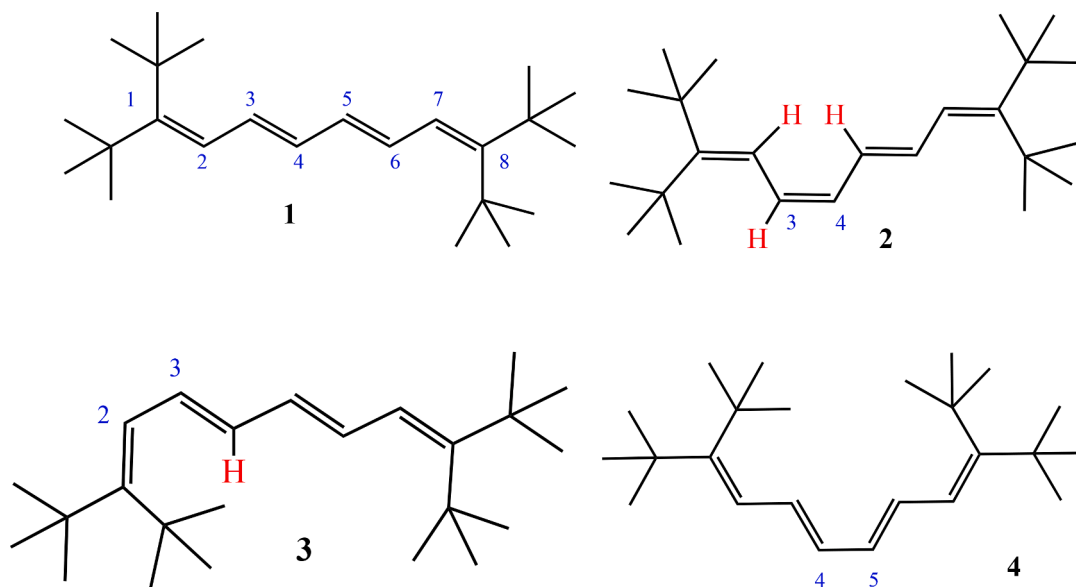


Fig. 6. Absorption and emission (fluorescence) spectra of 4tmC obtained at 77 K and exciting at 300 nm.

structure of 4tmC, therefore it is produced from the electronically excited state 1^1Bu . The emission from 440 nm on, is assigned to a molecular structure of 4tmC generated by the rotation of its polyenic chain. Later we will try to make this assignment more concrete with the help of theoretical calculations.

In Fig. 6 we compare the absorption and emission spectra of 4tmC recorded at 77 K. We can conclude that: i) there is no Stokes shift and ii) the structured emission in the range 340–440 nm compares well with the absorption spectrum and consequently we are faced with an emission generated from the 1^1Bu state of the compound.

In summary, all these experiments reveal that 4tmC i) has a planar structure in the ground state ii) shows two distinct fluorescence bands: one between 340 and 440 nm, that can be assigned to the *all-trans* form of the compound and another band (>440 nm) due to a different structure of ttBP4 iii) this new structure is generated by a rotation of its polyene chain in the electronic excited state iv) the torsion takes place



Scheme 2. The four possible rotated structures of ttbP4.

within the crystalline structure, that is, in a medium in which there is a strong structural constriction. While it is not our aim to study the mechanism through which the molecule rotates, we want to note that there are different mechanisms proposed in the literature to explain torsion in condensed phase, such as one-bond flip (OBF, also known as the double-bond twist), volume-conserving hula-twist (HT) and the bicycle pedal (BP) mechanisms [35]. Some examples of this torsions in condensed phases are the BP mechanism observed in crystalline butadienes [36–39], hexatrienes [40,41] and photoactive yellow protein [42] and has been implicated in the visual retinoid cycle [11].

It is also important to point out that the rotated structure is preserved in the crystal for a time once ttbP4 has returned to its ground electronic state. Let us recall that its excitation spectrum (Fig. 5) is structured and significantly red shifted with respect to the absorption spectrum of the compound. Also, it is important to note that the peaks that appear in the

excitation spectrum at wavelengths greater than 360 nm (Fig. 5) coincide with the small absorption bands observed in the absorption spectra of 4tmC (Fig. 1a). These signals must be attributed to the fact that some rotated molecules are temporarily trapped in the crystal. In a 4tmC sample that has not been previously illuminated, these small absorptions are virtually undetectable.

3.2. On the rotation of the polyene chain of ttbP4

The most stable structure of ttbP4 in its ground electronic state is an all-*trans* (all single and double bonds present *trans* configuration) planar structure as shown by X-ray diffraction experiments [33]. This structure could rotate around a bond in the polyene chain in its electronic excited state. In this way, four possible structures can be generated: two *s-cis* isomers, by rotating around a double bond, structure 1 (C1-C2

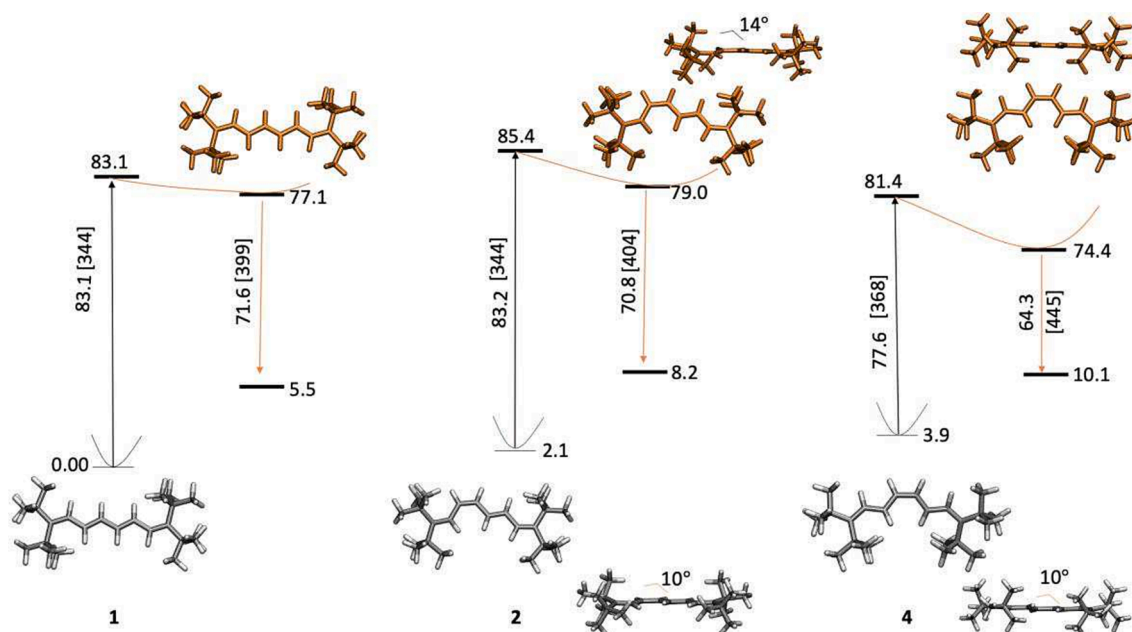


Fig. 7. Gas phase optimized geometries for structures 1, 2, and 4 of Scheme 2, both in their fundamental and first excited electronic states. The relative energies for each structure are shown together with the vertical transition energies. All energies are in kcal/mol. Energies in nm are shown between brackets [].

Table 2

Dipole moments of structures 1, 2 and 4 of ttbP4, both in its ground and first excited electronic states.

Structure	Ground state	1^1Bu state
1	0.000	0.000
2	0.407	0.749
4	0.457	0.651

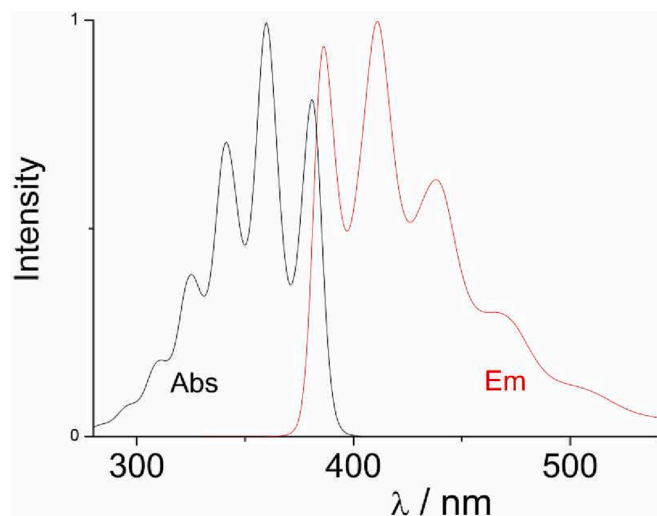


Fig. 8. Normalized simulated absorption and emission spectra for structure 1 of ttbP4 structure at $T = 293$ K. The simulation was done using adiabatic excitation energies.

bond) and structure 2 (C3-C4 bond) and two different *s-cis* conformers, by rotating around a single bond, structure 3 (C2-C3 bond) and 4 (C4-C5 bond). Scheme 2 shows the four structures. Note that structure 1 regenerates the starting *all-trans* structure of ttbP4, since rotation around C1-C2 double bond simply changes the two terminal *tert*-butyl groups to a fully equivalent position.

3.3. Theoretical contributions to the photophysics of ttbP4

Fig. 7 shows the optimized structures 1, 2, and 4 of ttbP4 in its ground and first excited electronic state. We were not able to optimize structure 3 since it converts back to structure 1 during optimization, probably due to the high steric hindrance between the hydrogen atom on C4 and one of C1 *tert*-butyl groups.

The *all-trans* structure 1 is the most stable of the three optimized structures, in agreement with experiments [33]. Structure 2 and 4 are ~ 2 and ~ 4 kcal/mol higher in energy, respectively.

Structure 1 is planar in the ground state, while 2 and 4 are slightly out of plane (10°) due to the steric repulsion between the hydrogen atoms on C2 and C5; and C3 and C6 of the polyene chain, respectively. On the other hand, structure 1 and 4 are planar in the 1st excited state, while structure 2 appears even more rotated than in its ground state (14° in the first excited state).

The computed dipole moments for each of the three structures in the ground and first excited state are reported in Table 2. It is interesting to note that while 1, the *all-trans*-planar structure is apolar both in the ground and excited state, structure 2 and 4 present a small dipole moment of 0.40 and 0.46 D in their ground state and slightly higher, 0.65 and 0.75 D, in their first electronically excited state, respectively.

The data in Table 2 allow us to deduce that the excited electronic state of structures 2 and 4 are slightly stabilized in the crystal with respect to that of structure 1, and therefore, except for problems due to

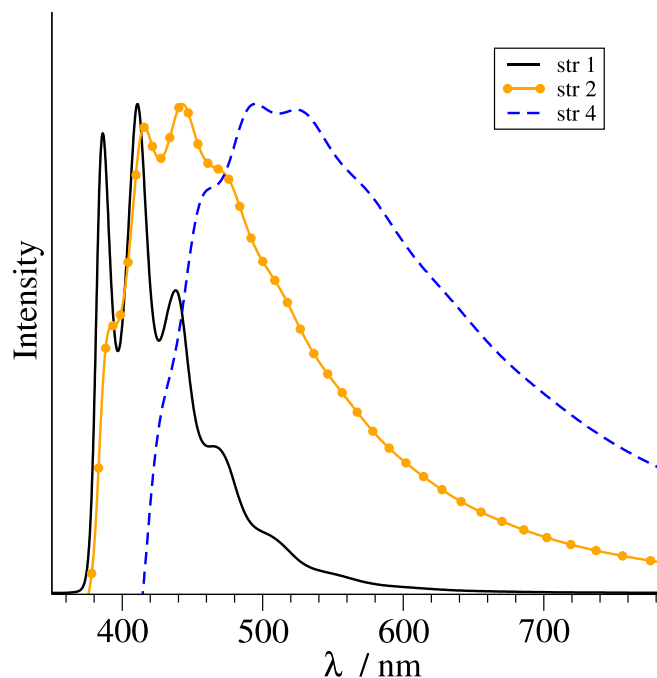


Fig. 9. Normalized simulated emission spectra for structures 1 (solid black line), 2 (orange circles) and 4 (dashed blue line) at temperature of 293 K. (For interpretation of the references to color in this figure legend, the reader is referred to the web version of this article.)

potential barriers, the excited sample of structure 1 will tend to rotate its polyene chain in the excited electronic state. However, due to the small values of the dipole moment shown in Table 2, it is expected that the energies of the transitions will hardly change when moving from the crystalline to the gas phase.

The values for the vertical emission of the three structures are collected in Fig. 7 (orange arrows). The emission from structures 1 and 2 should appear at the same wavelength, while the emission from structure 4 appears redshifted, in agreement with the experimental observation (see Figs. 3 and 4). Therefore, these values indicate that the photophysics of 4tmC could be largely described by structures 1 and 4.

To further investigate the origin of the two distinct fluorescence bands in ttbP4 fluorescence spectra, we simulated the absorption and emission spectra of the different structures of ttbP4 using FCclasses3 program [31]. This program allows to take into account vibronic transitions (simultaneous transitions between electronic and vibrational levels) reproducing the lineshape of the spectra at any temperature. In Fig. 8 we show the simulated absorption and emission spectra of structure 1 of ttbP4 at 293 K.

Comparing the computed emission spectra for ttbP4 structure 1 (Fig. 8) and the experimental spectra collected in Figs. 3 and 4 we can see that the structured band (340–440 nm) that appears in the emission of ttbP4 is generated by the transition from the excited state 1^1Bu , populated in the absorption process, back to the ground state.

To assign the second emission band (>440 nm) appearing in crystalline ttbP4 fluorescence spectra we computed the emission spectra of the three possible rotated structures at 293 K (Fig. 9: structure 1, in black, structure 2 (in orange and circles), and structure 4 (dashed blue line)). Recall that we were not able to optimize structure 3. It is evident from Fig. 9, comparing with the experimental emission spectra (Figs. 3 and 4) that the two fluorescence bands detected in 4tmC correspond to the fluorescence generated by structures 1 and 4. The simulated spectra show that the emission from structures 1 and 4 recovers the shape and position of the two emission bands appearing in the experimental spectra. The presence of structure 2 is also discarded by these results, since the emission from structure 2 will overlap with emission from

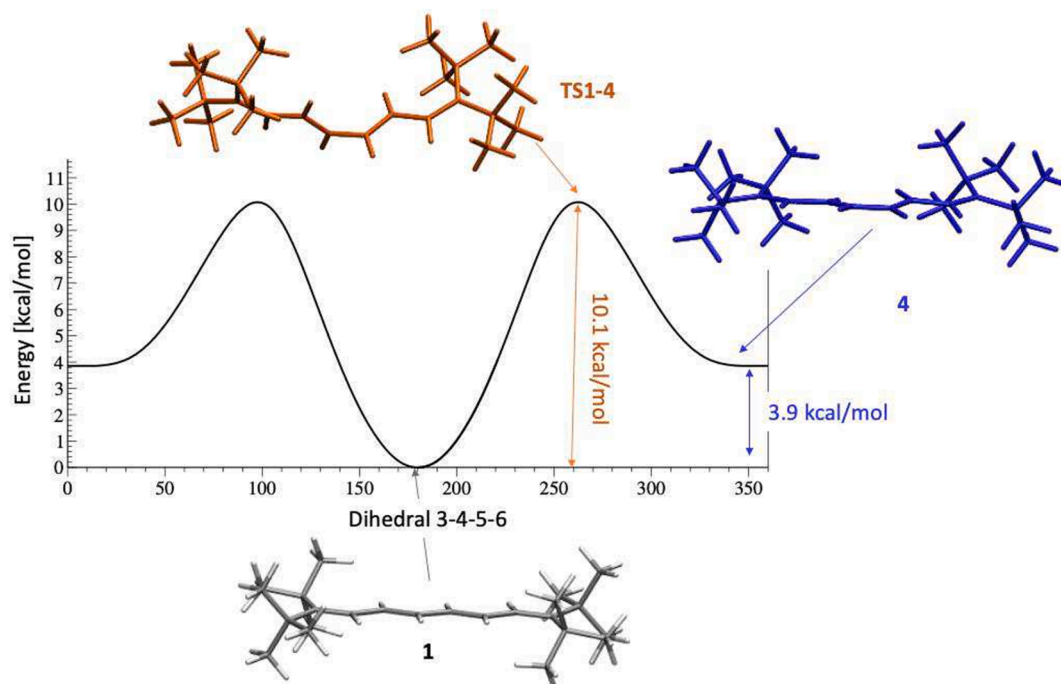


Fig. 10. Ground state energy profile for the rotation around the C4-C5 single bond that connects structure **1** (all-trans) with rotated structure **4**. The optimized geometries for relevant structures are also shown.

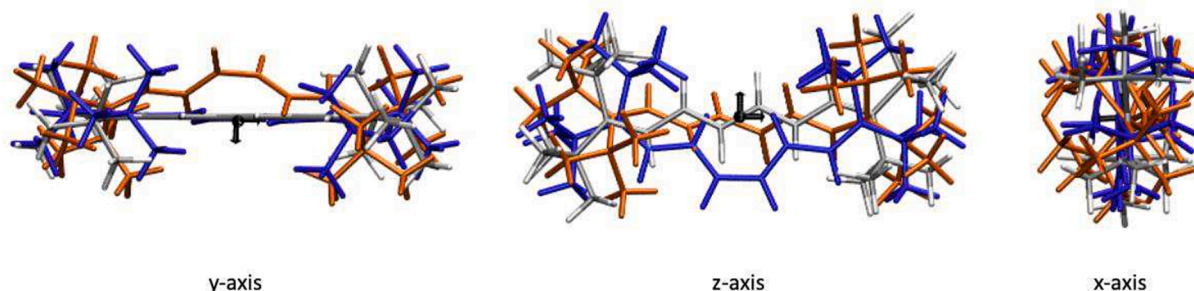


Fig. 11. View of the three structures superimposed along the three different axes. Gray: all-trans (**1**); blue (structure **4**) and orange: ground state **TS1-4** linking the two structures. (For interpretation of the references to color in this figure legend, the reader is referred to the web version of this article.)

structure **1** making the structure of the first band disappear.

3.4. Assessing the possibility of rotation in the crystal phase

As previously stated, it is not our aim to study the mechanism for this torsion on the excited state. Several previous studies propose different mechanisms to explain cis/trans isomerization of similar molecules in an environment as spatially restricted as the solid phase or a protein cavity upon light absorption [35–43]. In order to provide further evidence that the reversible isomerization in the solid phase is possible we show in Fig. 10 the ground state energy profile for this rotation.

The computed energy barrier for the torsion is 10.1 kcal/mol and the corresponding TS structure, **TS1-4**, is shown in orange in Fig. 10. If we look at Fig. 7 (right side), we see that the excited state minimum of **4**, after emitting (Franck-Condon region), has a ground state energy of 10.1 kcal/mol. Therefore, the molecule would have energy enough to overcome the torsional barrier. However, we should keep in mind that these calculations are done in the gas-phase, and the process would take place in the more hindered solid phase.

As a way of assessing the volume change along this torsion coordinate, we show in Fig. 11 the optimized geometries, superimposed, of the all-trans structure, **1**, the rotated structure along the middle single bond,

Table 3

Rotational constants (GHz) and moments of inertia (kg m^2) for structure **1** (all-trans), structure **4** and the transition state (**TS1-4**) linking the two structures.

	all-trans (str1)		str4		TS1-4	
	Rot Cont. [GHz]	I [kgm^2]	Rot Cont. [GHz]	I [kgm^2]	Rot Cont. [GHz]	I [kgm^2]
A	0.50084	$1.68 \cdot 10^{-42}$	0.51057	$1.65 \cdot 10^{-42}$	0.49039	$1.71 \cdot 10^{-42}$
B	0.06638	$1.27 \cdot 10^{-41}$	0.07897	$1.06 \cdot 10^{-41}$	0.07002	$1.20 \cdot 10^{-41}$
C	0.06184	$1.36 \cdot 10^{-41}$	0.07306	$1.15 \cdot 10^{-41}$	0.06894	$1.22 \cdot 10^{-41}$

4, and the ground state transition state linking these two structures, **TS1-4**.

Looking Fig. 11, along y-axis we observe that structures **1** (all-trans) and **4** are coplanar (**4** is slightly out of plane, see Fig. 7), with the bulky *tert*-butyl groups occupying most of the volume. The polyene chain of **TS1-4** (orange) is clearly out of plane, but still it will only slightly surpass the volume occupied by the other two structures due to the size of the *tert*-butyl groups (see also x-axis perspective).

We also computed the moments of inertia for these three structures (see Table 3) as a measure of the size of each of them. Structure 4 has the smallest values of all of them (I_A , I_B and I_C), meaning that it is the most compact structure. On the other side, the all-trans structure (1) has the highest values for I_B and I_C meaning that is the structure that occupies a higher volume in the corresponding plane. The value of I_A for TS1-4 is slightly larger than the value for 1 and 2 so it would occupy a slightly larger volume on the corresponding direction, but the difference is small (2% larger than I_A for 1). TS1-4 will be the structure with the highest volume along the rotation pathway and is only slightly larger than the most-stable and original *all-trans* structure 1. All these results point that the volume change along the torsional process is almost negligible and therefore it would be possible that the isomerization takes place in the solid phase.

4. Conclusions

When a single crystal of ttbP4 is electronically excited, it is evident that this compound is capable of efficiently rotating its polyene chain around its second carbon-carbon single bond (C4-C5), in a molecular environment as hindered as the crystalline phase. After emission, the rotated structure remains trapped for a while in the ground state and eventually converts back to the original *all-trans*-form of the compound.

We have shown, by combining experimental and theoretical results, that the fluorescent emission of the ttbP4 crystal is the sum of two emissions, a structured one that is generated from the 1^1Bu state and a non-structured redshifted one that is generated from the rotated form of the polyene compound. Theoretical calculations of the vibrationally resolved electronic absorption and emission spectra allowed us to identify the rotated structure as the one generated by the torsion around the second single bond (C4-C5 bond, structure 4) of ttbP4.

These results can be considered as evidence to rationalize the proposed mechanism of vision.

CCRediT authorship contribution statement

Javier Catalán: Writing – review & editing, Writing – original draft, Methodology, Investigation, Formal analysis, Data curation, Conceptualization. **Ana Martín-Somer:** Writing – review & editing, Writing – original draft, Methodology, Investigation, Formal analysis. **Henning Hopf:** Investigation, Methodology.

Declaration of Competing Interest

The authors declare that they have no known competing financial interests or personal relationships that could have appeared to influence the work reported in this paper.

Data availability

Data will be made available on request.

Acknowledgements

Javier Catalán, Emeritus Professor, is thankful to the Universidad Autónoma de Madrid for providing the facility to carry out this research. A.M.S. thanks the CCC-UAM for generous allocation of computing time and the Madrid Government (Comunidad de Madrid-Spain) under the Multiannual Agreement with UAM in the line Support to Young Researchers, in the context of the V PRICIT (SI3-PJI-2021-00463). We acknowledge Javier Cerezo for fruitful discussions and providing help with FCclasses3 program to simulate the spectra.

References

- [1] E. W. Abrahamson, S.E. Ostroy, The Photochemical Macromolecular Aspects of Vision, in Progress in Biophysical and Molecular Biology, Vol 7, Edited by J.A.V. Butler nad H.E. Huxley, Pergamon, Oxford, 1967.
- [2] M.L. Applebury, P.A. Hargrave, Vision Res. 1986 (1881) 26.
- [3] R.R. Birge, Ann. Rev. Phys. Chem. 41 (1990) 684.
- [4] R.J. Cogdell, H.A. Frank, Biochim. Biophys. Acta 895 (1987) 63.
- [5] D. Siefermann-Harms, Biochim. Biophys. Acta, 1085, 811, 325.
- [6] C.O. Chichester, T.M.O. Nakayama, in Biogenesis of Natural Products, Edited by P. Bernfeld, Pergamon, Pxford, 1963.
- [7] R. Edge, T. Truscott, Antioxidants 7 (2018) 5.
- [8] A. J. Young, L.L. Gordon, 2018, 7, 28.
- [9] G.N. Lewis, M. Calvin, Chem. Rev. 25 (1939) 273.
- [10] A. Maccoll, Quart. Rev. Chem. Soc. 1 (1947) 136.
- [11] A. Warshel, Nature(London) 1976, 260, 679.
- [12] R.S.H. Liu, A.E. Asato, Proc. Nat. Acad. Natl. Acad. Sci. U.S.A. 82 (1985) 259.
- [13] R.S.H. Liu, G.S. Hammond, Proc. Nat. Acad. Natl. Acad. Sci. U.S.A., 2000, 97, 11153. ; Chem. Eur. J. 2001, 7, 4537. ; Photochem. Photobiol., 2003, 2, 835.
- [14] R. Hubbard, G. Wald, j. Gen. Physiol. 36 (1968) 673.
- [15] A. Warshel, M. Karplus, J. Am. Chem. Soc. 96 (1974) 5577.
- [16] B. Honig, A. Warshel, M. karplus, Acc. Chem. Res. 1975, 8, 92.
- [17] A. Warshel, Proc. Natl. Acad. Sci. USA 75 (1978) 2558.
- [18] R.S. Mulliken, J. Chem. Phys. 7 (1939) 364.
- [19] B.S. Hudson, B.E. Kohler, Chem. Phys. Lett. 14 (1972) 299.
- [20] J. Catalán, J. Phys. Org. Chem., 2021, 34, e4147. and referees therein.
- [21] J. Catalán, H. Hopf, Eur. J. Org. Chem. (2004) 4694.
- [22] J. Catalán, H. Hopf, C. Mlynec, D. Klein, P. Kilickiran, Chem. Eur. J. (2005) 3915.
- [23] J. Catalán, H. Hopf, D. Klein, M. Martus, J. Phys. Chem. B 112 (2008) 5653.
- [24] J. Catalán, H. Hopf, M. Martus, J. Chem. Phys. 128 (2008), 104504.
- [25] J. Catalán, P. Pérez, H. Hopf, D. Klein, J. Chem. Phys. 129 (2008), 014505.
- [26] D. Klein, P. Kilickiran, C. Mlynec, H. Hopf, I. Dix, P.G. Jones, Chem. Eur. J. 16 (2010) 10507.
- [27] J. Catalán, C. Díaz-Oliva, J.C. del Valle, Chem. Phys. 525 (2019), 110422.
- [28] C. Adamo, V. Barone, J. Chem. Phys. 110 (1999) 6158.
- [29] Gaussian 16, Revision A.03, M. J. Frisch, G. W. Trucks, H. B. Schlegel, G. E. Scuseria, M. A. Robb, J. R. Cheeseman, G. Scalmani, V. Barone, G. A. Petersson, H. Nakatsuji, X. Li, M. Caricato, A. V. Marenich, J. Bloino, B. G. Janesko, R. Gomperts, B. Mennucci, H. P. Hratchian, J. V. Ortiz, A. F. Izmaylov, J. L. Sonnenberg, D. Williams-Young, F. Ding, F. Lipparini, F. Egidi, J. Goings, B. Peng, A. Petrone, T. Henderson, D. Ranasinghe, V. G. Zakrzewski, J. Gao, N. Rega, G. Zheng, W. Liang, M. Hada, M. Ehara, K. Toyota, R. Fukuda, J. Hasegawa, M. Ishida, T. Nakajima, Y. Honda, O. Kitao, H. Nakai, T. Vreven, K. Throssell, J. A. Montgomery, Jr., J. E. Peralta, F. Ogliaro, M. J. Bearpark, J. J. Heyd, E. N. Brothers, K. N. Kudin, V. N. Staroverov, T. A. Keith, R. Kobayashi, J. Normand, K. Raghavachari, A. P. Rendell, J. C. Burant, S. S. Iyengar, J. Tomasi, M. Cossi, J. M. Millam, M. Klene, C. Adamo, R. Cammi, J. W. Ochterski, R. L. Martin, K. Morokuma, O. Farkas, J. B. Foresman, and D. J. Fox, Gaussian, Inc., Wallingford CT, 2016.
- [30] F. Santoro, R. Improtà, A. Lami, V. Barone, J. Chem. Phys. 126 (2007), 184102.
- [31] J. Cerezo, F. Santoro, J. Comput. Chem. (2022) 1, <https://doi.org/10.1002/jcc.27027>.
- [32] C. Benzi, V. Barone, R. Tarroni, C. Zannoni, J. Chem. Phys. 125 (2006), 174904.
- [33] D. Klein, Ph.D. dissertation, Braunschweig, 2000.
- [34] R.M. Gavin, C. Weisman, J.K. Mc Vey, S.A. Rice, J. Chem. Phys. 68 (1978) 522.
- [35] R.S.H. Liu, L.-Y. Yang, J. Liu, Mechanisms of Photo- isomerization of Polyenes in Confined Media: From Organic Glasses to Protein Binding Cavities, Photochem. Photobiol. 83 (2007) 2–10.
- [36] C.R. Aldaz, T.J. Martinez, and P. M. Zimmerman J. Phys. Chem. A 124 (2020) 8897–8906.
- [37] D. Furukawa, S. Kobatake, A. Matsumoto, Direct observation of change in the molecular structure of benzyl (Z, Z)-muconate during photoisomerization in the solid state, Chem. Commun. 1 (2008) 55–57.
- [38] T. Odani, A. Matsumoto, K. Sada, M. Miyata, One-WayEZ- isomerization of bis(n-butylammonium) (Z, Z)-muconate under photoirradiation in the crystalline state, Chem. Commun. 19 (2001) 2004–2005.
- [39] J. Saltiel, M.A. Bremer, S. Laohasurayotin, T.S.R. Krishna, Photoisomerization of Cis, Cis- and Cis, Trans-1,4-Di-o-Tolyl-1,3- butadiene in glassy media at 77 K: one-bond-twist and bicycle- pedal mechanisms, Angew. Chem., Int. Ed. 47 (2008) 1237–1240.
- [40] F. Tong, M. Al-Haidar, L. Zhu, R.O. Al-Kaysi, C.J. Bardeen, Photoinduced peeling of molecular crystals, Chem. Commun. 55 (2019) 3709–3712.
- [41] Y. Sonoda, Y. Kawanishi, S. Tsuzuki, M. Goto, Crystalline-state Z, E- photoisomerization of a series of (Z, E, Z)-1,6-diphenyl- hexa-1,3,5-triene 4,4'-dicarboxylic acid dialkyl esters. Chain length effects on the crystal structure and photoreactivity, J. Org. Chem. 70 (2005) 9755–9763.
- [42] J. Saltiel, C.E. Redwood, K. Laohasurayotin, R. Samudrala, Photochemistry of the 1,6-dideuterio-1,3,5-hexatrienes in solution: efficient terminal bond photoisomerization in one-bond-twist and bicycle pedal ways, J. Phys. Chem. A 122 (2018) 8477–8489.
- [43] Y.O. Jung, J.H. Lee, J. Kim, M. Schmidt, K. Moffat, V. Šrajcar, H. Ihee, Volume-conserving trans-cis isomerization pathways in photoactive yellow protein visualized by picosecond X-ray crystallography, Nat. Chem. 5 (2013) 212–220.